Ultrasensitive Electroanalysis of Low-Level Free MicroRNAs in Blood by Maximum Signal Amplification of Catalytic Silver Deposition Using Alkaline Phosphatase-Incorporated Gold Nano...

ARTICLE *in* ANALYTICAL CHEMISTRY · SEPTEMBER 2014

Impact Factor: 5.64 · DOI: 10.1021/ac5028885 · Source: PubMed

7 AUTHORS, INCLUDING:

Hua Wang
Qufu Normal University
164 PUBLICATIONS **1,857** CITATIONS

SEE PROFILE

analytical chemistry

Article

pubs.acs.org/ac

Ultrasensitive Electroanalysis of Low-Level Free MicroRNAs in Blood by Maximum Signal Amplification of Catalytic Silver Deposition Using Alkaline Phosphatase-Incorporated Gold Nanoclusters

Yanmei Si,[†] Zongzhao Sun,[†] Ning Zhang,[†] Wei Qi,[†] Shuying Li,[†] Lijun Chen,[‡] and Hua Wang*[,†]

[†]Shandong Province Key Laboratory of Life-Organic Analysis, College of Chemistry and Chemical Engineering, Qufu Normal University, Qufu City, Shandong Province 273165, P. R. China

[‡]Hospital of University, Qufu Normal University, Qufu City, Shandong Province 273165, P. R. China

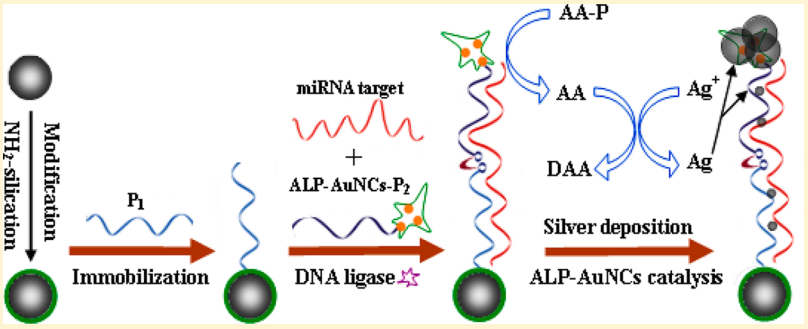

ABSTRACT: An ultrasensitive sandwich-type analysis method has been initially developed for probing low-level free microRNAs (miRNAs) in blood by a maximal signal amplification protocol of catalytic silver deposition. Gold nanoclusters (AuNCs) were first synthesized and in-site incorporated into alkaline phosphatase (ALP) to form the ALP-AuNCs. Unexpectedly, the so incorporated AuNCs could dramatically enhance the catalysis activities of ALP-AuNCs versus native ALP. A sandwiched hybridization protocol was then proposed using ALP-AuNCs as the catalytic labels of the DNA detection probes for targeting miRNAs that were magnetically caught from blood samples by DNA capture probes, followed by the catalytic ligation of two DNA probes complementary to the targets. Herein, the ALP-AuNC labels could act as the bicatalysts separately in the ALP-catalyzed substrate dephosphorylation reaction and the AuNCs-accelerated silver deposition reaction. The signal amplification of ALP-AuNCs-catalyzed silver deposition was thereby maximized to be measured by the electrochemical outputs. The developed electroanalysis strategy could allow for the ultrasensitive detection of free miRNAs in blood with the detection limit as low as 21.5 aM, including the accurate identification of single-base mutant levels in miRNAs. Such a sandwich-type analysis method may circumvent the bottlenecks of the current detection techniques in probing short-chain miRNAs. It would be tailored as an ultrasensitive detection candidate for low-level free miRNAs in blood toward the diagnosis of cancer and the warning or monitoring of cancer metastasis in the clinical laboratory.

MicroRNAs (miRNAs), which can regulate the expression of genes in plants and animals, comprise a class of noncoding 18−25 nucleotides.[1] Since miRNAs can regulate genes that are associated with human cancers, neurological diseases, and viral infections, they can act as the useful diagnostic and prognostic biomarkers for the basic biomedical research and evaluations.[2] In particular, the expressing levels of miRNAs in peripheral blood have been well established to be the sensitive biomarkers for cancer diagnostics and blood-way metastasis.[3−7] The profiling or quantification of free miRNAs in blood, however, can be challenged by the complicated background interference, exceptionally by the short chains, similar nucleotide sequences, and low expression levels of miRNAs in blood.[8]

In recent years, many modern analytical methods have been established to quantify DNAs and RNAs, such as reverse transcription polymerase chain reaction (RT-PCR),[9] surface enhanced Raman spectroscopy,[10] and enzyme-catalytic amplification technology.[11−15] Gracefully successive as these methods are, they may suffer from some shortcomings such as large expensive equipment, precise temperature controls, time-consuming procedures, and well-trained personnel.[16] In particular, some of these methods may be suitably used only for targeting nucleotides with long nucleotide chains. For example, the sandwiched enzyme-catalytic amplification technology may be trapped in the detection of miRNAs, because the hybridized double chains, formed either between targets and the capture probes or between targets and the detection probes, can have too low chain-melting temperature and strength to withstand the large signal amplification, resulting in the low sensitivity of

Received: August 1, 2014
Accepted: September 20, 2014
Published: September 20, 2014

   dx.doi.org/10.1021/ac5028885 | *Anal. Chem.* 2014, 86, 10406−10414

miRNA analysis. Therefore, the development of an ultrasensitive detection candidate for the analysis of low-level miRNAs in media like blood has been a challenging but attractive issue to date.

Moreover, alkaline phosphatase (ALP) has been commonly used in the enzyme-catalytic amplification technologies for detecting proteins and genes.[17−19] The products of ALP catalytic hydrolysis reactions from the substrates such as ascorbic acid 2-phosphate (AA-p) can serve as the reducing agents in the silver deposition for amplifying signals toward sensitive gene assays.[11,12,15] For example, Yu's group has reported the detection of point mutation of DNAs by monitoring the accumulation of silver reduced by ALP catalysis-produced ascorbic acid (AA).[15] Moreover, the gold-accelerated silver deposition technique, known as the gold−silver staining strategy, has been well recognized to be a sensitive analysis procedure, combined with optical[20] or electrochemical[14] measurements, in biomedical imaging and bioanalysis fields.[21] Wonderful work was done in Willner's group, where enzymes (i.e., ALP) were modified with ultrasmall gold nanoparticles (AuNPs) as "biocatalytic ink" for the silver deposition to grow metallic nanowires.[22] Moreover, Ju and co-workers utilized ALP-labeled antibody to functionalize AuNPs toward a sandwich-type immunoassay for human IgGs based on the gold-accelerated deposition of silver.[14] Nevertheless, most enzyme catalysis-based detection procedures reported to date may still suffer from the limited catalysis activity of enzyme for signal amplification.

It is well-known that the catalysis active centers of enzymes are mostly located at their protein pockets.[23−25] For example, ALP, a homodimeric enzyme that catalyzes the hydrolysis and transphosphorylation of phosphate monoesters, can possess the catalytic active-site pocket with the conformation of the Ser102 nucleophile and the metal-binding occupancy.[24,25] In recent decades, increasing attention has been paid to the use of nanomaterials (i.e., AuNPs and carbon nanotubes) to label enzymes to access these catalytic active-site pockets of enzymes for enhancing their catalysis, especially electrocatalysis.[26−28] Additionally, some noble metal nanomaterials intrinsically possess catalytic activities substantially, depending on their sizes, known as the "size effects". For example, AuNPs with sizes smaller than 5.0 nm can present high catalytic activity.[29−31] Therefore, the synthesis and applications of size-reducing or ultrasmall noble metal nanoparticles, i.e., gold nanoclusters (AuNCs) to replace AuNPs for more improved enzyme catalysis and gold-catalytic silver deposition reactions, are of great interest.

In this work, AuNCs were initially synthesized and in-site incorporated into the protein matrix of ALP, as an example of enzyme with the catalysis under alkaline environment, by the protein-based biomineralization route.[32] The resulting ALP-incorporated AuNCs (ALP-AuNCs) would obtain dramatically enhanced catalysis activity. On the other hand, the AuNCs could act as the gold catalyst to accelerate the silver deposition reaction. The bicatalysis performances of ALP-AuNCs were verified colorimetrically and electrochemically in the catalytic dephosphorylation and the silver deposition reactions compared to native ALP. Furthermore, ALP-AuNCs were employed as the bicatalytic labels of DNA detection probes for the sandwiched detection of short-chain miRNAs that were captured by the magnetic particles-loaded DNA capture probes. The ligation of two DNA probes complementary to the targets was then conducted to increase the bearing strength and capacity of ALP-AuNCs-labeled DNA detection probes for the more enlarged silver deposition and accumulation, leading to a maximum amplification of silver signal. Investigation results indicate that the developed analysis method can allow for the ultrasensitive and selective quantification of miRNAs with low levels in blood including their single-base mutant levels, showing the feasibility of being applied for the clinical diagnostics and warning of cancer and cancer metastasis.

EXPERIMENTAL SECTION

Materials and Reagents. Alkaline phosphatase (ALP) was purchased from New England Biotechnology (Beijing, China). 4-Nitrophenyl phosphate (pNPP) disodium was obtained from Solarbio (Beijing, China). Bovine serum albumin (BSA), chlorauric acid ($HAuCl_4{\cdot}3H_2O$), silver nitrate ($AgNO_3$), glutaraldehyde, trihydroxymethyl aminomethane (Tris), (3-aminopropyl) triethoxysilane, ethanolamine, and glycine were purchased from Sinopharm Chemical Reagent Co. (China). Ascorbic acid 2-phosphate (AA-p) and cetyltrimethylammonium bromide (CTAB) were provided by Dibai Reagents (Shandong, China). The blood samples were kindly provided by the local hospital. All other reagents were of analytical grade. Deionized water (>18 MΩ) was supplied from an Ultrapure water system (Pall, USA). DNA ligase containing ligation buffer, amine-functionalized oligonucleotides of DNA capture and detection probes, wild (matched) miRNAs and single-base mutant (mismatched) miRNAs were synthesized by Takara Biotechnology (Dalian) Co., Ltd., including: (1) DNA capture probe: 5′-Amine-AAC TAT ACA AC-3′; (2) DNA detection probe: 5′-CTA CTA CCT CA-amine-3′; (3) Wild miRNA: 5′-UGA GGU AGU AGG UUG UAU AGU U-3′; (4) Single-based mutant miRNA: 5′-UGA GGU AGU A<u>C</u>G UUG UAU AGU U-3′.

Buffer solutions include the hybridization buffer (pH 7.4) consisting of 10 mM Tris-HCl, 1.0 mM EDTA, 1.0 mM CTAB, and 0.50 M NaCl; the DNA rinsing buffer (pH 7.4) composed of 100 mM NaCl and 10 mM Tris-HCl; the ligation buffer (pH 7.4) containing 30 mM Tris-HCl, 1.0 mM $MgCl_2$, 10 mM DTT, and 1.0 mM ATP; the silver deposition substrate (pH 9.8) consisting of 3.5 mM AA-p, 2.0 mM $AgNO_3$, and 2.0 mM $Mg(NO_3)_2$ in glycine buffer.

Electrochemical measurements were conducted with an electrochemical workstation CHI760D (CH Instrument, Shanghai, China) connected to a personal computer. A three-electrode system was applied consisting of magnetic glassy carbon working electrode (Incole Union Technology, Tianjin, China), a Pt wire counter electrode, and an Ag/AgCl reference electrode. The investigation of enzyme activities was operated by a microplate reader (Infinite M 200 PRO, Tecan, Austria) and 96-well plates (JET BIOFIL, Guangzhou, China). Characterizations of the as-prepared products were performed by using transmission electron microscopy (TEM, FEI Tecnai G20, USA) operated at 100 kV.

Synthesis and Characterization of ALP-AuNCs. The synthesis of ALP-AuNCs was conducted following a modified protein-based biomineralization route.[32] All glassware was first washed with nitro-hydrochloric acid (HNO_3/HCl volume ratio = 1:3) and then rinsed with ethanol and ultrapure water. In a typical experiment, 4.4 mL of $HAuCl_4$ solution (10 mM) was mixed with the BSA solution (4.4 mL, 50 mg/mL). Under vigorous stirring, an aliquot of 0.20 mL of NaOH solution (1.0 M) was then dropped into the mixture to be stirred for 1 h. Furthermore, 1.0 mL of ALP (100 U/mL) was introduced into

dx.doi.org/10.1021/ac5028885 | Anal. Chem. 2014, 86, 10406−10414

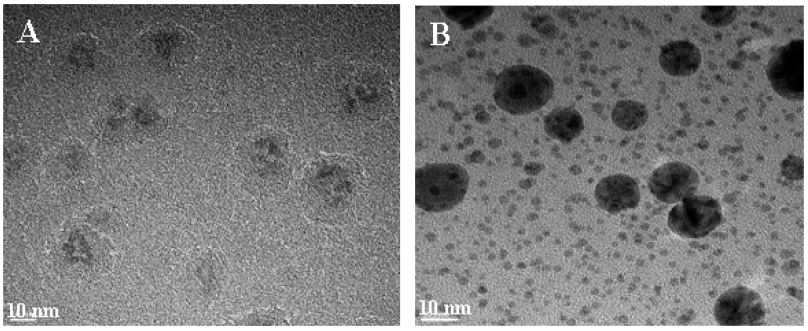

Figure 1. TEM images for (A) the as-prepared ALP-AuNCs and (B) the product of silver deposition reaction using ALP-AuNCs and the silver deposition substrate.

the mixing solution, and the reaction was allowed to proceed at 37 °C overnight. The resulting ALP-AuNCs product was subsequently dialyzed at 4 °C overnight to be stored for future use. Additionally, TEM images were obtained to characterize the ALP-AuNCs solution before and after the catalytic silver deposition.

Investigation of the Bicatalysis Activities of ALP-AuNCs. The catalysis activity of the prepared ALP-AuNCs for catalyzing dephosphorylation reaction of pNPP was investigated by colorimetric tests using a microplate reader and 96-well plates. An aliquot of ALP-AuNCs of different concentrations from 0.0125 to 0.125 U/mL was separately added to the reaction substrate containing 0.25 mM pNPP and 2.0 mM $Mg(NO_3)_2$ in carbonate buffer (pH 10.4) to react at 37 °C for 20 min. After being terminated with 2.0 M NaOH, the reactive products of *p*-nitrophenol (pNP) were measured at 405 nm and the absorbance intensities were recorded. Meanwhile, control experiments for the catalytic activity of ALP were conducted accordingly.

Furthermore, the catalytic performances of ALP-AuNCs were explored for silver deposition reactions compared to native ALP by using AA-p and $AgNO_3$ substrates. An aliquot of ALP-AuNCs of different concentrations was introduced to the silver deposition substrate (pH 9.8) containing 5.0 mM AA-p and 4.0 mM $AgNO_3$ in glycine buffer to react for 10 min in dark. Control experiments with ALP were also operated in the same way.

Preparation of Magnetic Particles-Loaded DNA Capture Probes. Fe_3O_4 particles were prepared according to a modified synthesis procedure reported previously.[33] These magnetic particles were then derivatized with amine group by the silication chemistry using (3-aminopropyl) triethoxysilane.[34,35] Furthermore, the amino-functionalized Fe_3O_4 particles (about 500 nm in diameter), washed twice with carbonate buffers (pH 8.5), were activated in 5.0% glutaraldehyde solution for 1 h, followed by washing. Thereafter, the activated magnetic particles were mixed with amine-derivatized DNA capture probes to be incubated for 1 h. After being washed twice, the modified particles were added into the blocking solution containing 1.0 mM ethanolamine and 0.10% BSA for 1 h and then washed twice. The so obtained magnetic particles-loaded DNA capture probes (Fe_3O_4-P_1) were subsequently stored at 4 °C for future use.

Synthesis of ALP-AuNCs-Labeled DNA Detection Probes. The modification of ALP-AuNCs on the amino-derivatized DNA detection probes was performed by the cross-linking chemistry with glutaraldehyde. Amine-derivatized DNA detection probes (1.0 μM) and ALP-AuNCs (10 U/mL) were first added to 5.0% glutaraldehyde solution for 1 h. Following that, the blocking solution containing 1.0 mM ethanolamine and 0.10% BSA was introduced to react for 1 h. Subsequently, the mixture was dialyzed at 4 °C overnight. The so formed ALP-AuNCs-modified DNA detection probes (ALP-AuNCs-P_2) were stored at 4 °C for future use. According to the same procedure, ALP-modified detection probes were prepared for the control tests.

Electrochemical Detection of miRNAs Based on the Catalytic Silver Deposition. An aliquot of magnetic particles-loaded capture probes (1.0 mg/mL particles) was separately added to the hybridization buffer containing complementary miRNAs with different concentrations ranging from 0.0050 to 20.0 fM in buffer or from 0.010 to 19.0 fM in blood. Following that, an aliquot of ALP-AuNCs-modified detection probes (1.0 μM probes) was introduced. The hybridization reactions were conducted with slow rotation at 15 °C for 50 min and then magnetically separated. DNA ligase (0.50 U/μL) was then introduced to catalyze the linking of two DNA probes in the ligation buffer for 2 h at 15 °C. After magnetic separation, the resulting suspension was incubated for 5 min at 37 °C and then washed twice with the DNA rinsing buffer. Furthermore, the suspension was added to the silver deposition substrate to be incubated for 10 min in the dark. After the magnetic separation and washing, an aliquot of 4.0 μL of the reactant product (1.0 mg/mL particles) was added to the surface of magnetic gold electrode for electrochemical measurements, of which the electrode was first polished with alumina powder and then ultrasonically cleaned with water and alcohol to be further dried under nitrogen stream. In addition, by following the same procedure above, the mutant-level identification experiments were conducted for the mutant miRNAs with different concentrations (0.50 to 18.5 fM) spiked in the wild miRNA samples at the fixed total miRNAs of 20.0 fM.

Throughout the electrochemical experiments, linear sweep voltammetry (LSV) was separately performed for the resulting electrodes in 1.0 M KCl solution over the potential range of -0.20−0.70 V at a scanning speed of 100 mV/s. A baseline correction of the resulting Ag/AgCl solid-state voltammograms was conducted with the CHI software.

RESULTS AND DISCUSSION

Preparation and Characterization of ALP-AuNCs with Bicatalysis Activities for the Silver Deposition Amplification. In this work, we have tried to synthesize and in-site incorporate AuNCs into the protein matrix of ALP, an enzyme model with catalysis under alkaline environment, by using a protein-scaffold biomineralization route.[32] Under the alkaline

dx.doi.org/10.1021/ac5028885 | *Anal. Chem.* 2014, 86, 10406−10414

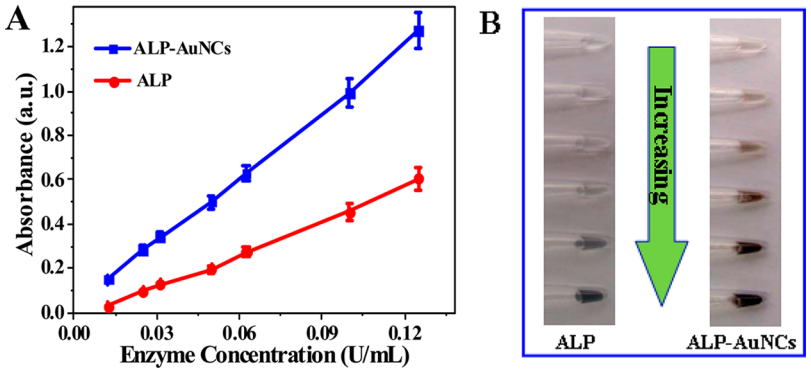

Figure 2. Colorimetric comparison of catalysis activities between ALP-AuNCs and native ALP of different concentrations in the dephosphorylation reactions of (A) pNPP substrate and (B) AA-p substrate with the photographs of the eventual products of the silver deposition reactions.

Scheme 1. (A) Schematic Illustration of the Principle for the Sandwich-Type Electroanalysis of miRNAs Using Magnetic Particles-Loaded DNA Capture Probe (Fe_3O_4-P_1) and ALP-AuNCs-Labeled DNA Detection Probe (ALP-AuNCs-P_2), Including the Ligase-Catalyzed Linking of Two DNA Probes and the ALP-AuNCs-Catalyzed Silver Deposition. (B) Schematic Illustration of the Magnetic Field-Aided Electroanalysis Procedure for miRNAs with the Amplification Signal of Silver Deposition Catalyzed by ALP-AuNCs

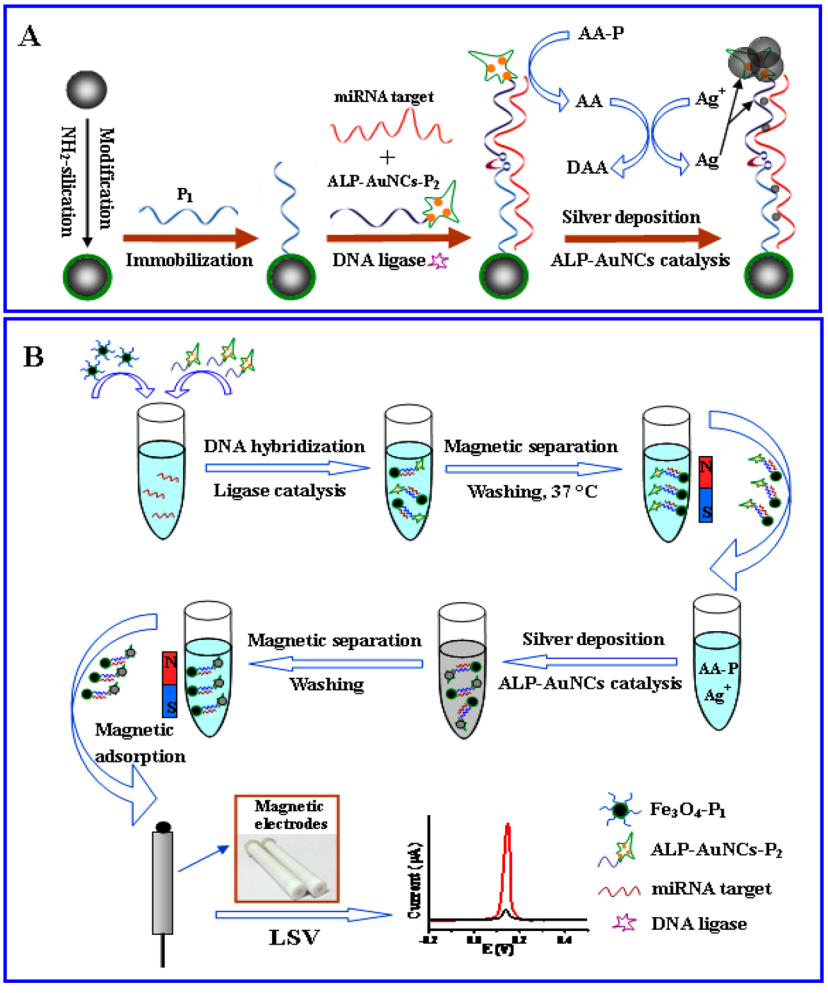

conditions, a slightly conformational denaturation of ALP protein might occur, so that the entrance paths of protein pockets of ALP could become more accessible. As a result, Au(III) ions could access the catalytic active-sites of ALP proteins to in situ form AuNCs reduced by some protein residues of the enzyme (e.g., tyrosine and cysteine),[32] resulting in ALP-incorporated AuNCs. The prepared ALP-AuNCs were characterized by TEM imaging (Figure 1A). One can note that ALP-AuNCs, in which ALP protein was stained by AuNCs (black coagulation), could be witnessed in the high-concentration protein matrix (white halo). The average coverage (loading) of ALP with AuNCs corresponds to about 12 per enzyme unit, estimated according to the similar method documented.[22,36] Figure 1B shows the TEM images for the

dx.doi.org/10.1021/ac5028885 | *Anal. Chem.* 2014, 86, 10406−10414

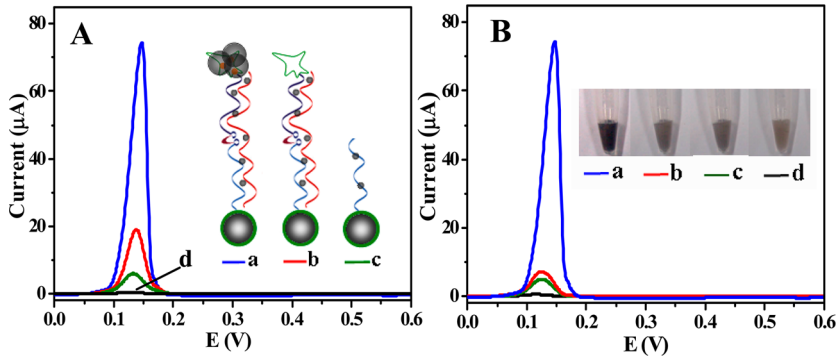

Figure 3. (A) Comparison of electrochemical LSV responses to miRNA targets (12.5 fM) between (a) ALP-AuNCs and (b) ALP-labeled DNA detection probes with the ligation of probes, (c) the ALP-AuNCs-based analysis without the ligation of probes, and (d) the control, corresponding to the products schematically illustrated (inset). (B) Electrochemical responses to (a) matched miRNAs (12.5 fM), (b) single-base mutant miRNAs (12.5 fM), (c) no target, and (d) the control, corresponding to the photographs of the product suspensions of silver deposition reactions (inset).

products of ALP-AuNCs-catalyzed dephosphorylation followed by the eventual silver deposition reactions. Obviously, silver layers could be deposited by the enzyme-induced metallization in the silver deposition substrate and then grow around ALP-AuNCs with different aggregation degrees.

A colorimetric comparison of the catalysis activities between ALP-AuNCs and native ALP was conducted in the dephosphorylation reactions using different concentrations of enzymes and the fixed concentration of two phosphorylated substrates (Figure 2). As is shown in Figure 2A, the catalysis activity of ALP-AuNCs is much higher than native ALP over the whole range of catalyst concentrations in catalyzing the pNPP reactions. Compared with native ALP, accordingly, ALP-AuNCs could present greatly enhanced catalysis activity, in contrast to the ALP modified with ultrasmall AuNPs showing unaltered catalysis activity.[22] The detailed mechanism for the enhanced catalysis of ALP-AuNCs, however, should be investigated in the future work. Furthermore, the catalysis capabilities of ALP-AuNCs were investigated comparably in catalyzing the dephosphorylation of AA-p substrate to generate reductive AA for the silver deposition reactions (Figure 2B). It was found that the silver amounts yielded for ALP-AuNCs are much more than those for native ALP, as evidenced by the visible color densities of reaction products. Herein, AuNCs in ALP-AuNCs should accelerate the silver deposition reaction. Therefore, ALP-AuNCs should serve as the bicatalyst combining the ALP catalyst in the dephosphorylation reaction and AuNCs catalyst in the silver deposition reaction. A silver deposition-based signal amplification method could thus be expected by using ALP-AuNCs as the labels of DNA probes for determining the low-level miRNAs, as demonstrated afterward.

Principle and Procedure for the Sandwich-Type Detection of miRNAs Based on the ALP-AuNCs-Catalyzed Silver Signal Amplification. The principle and analysis procedure of the sandwich-type sensing protocol for miRNAs is schematically illustrated in Scheme 1, including the sandwich-type hybridization, ligase-catalyzed linking, ALP-AuNCs-catalyzed dephosphorylation, and silver deposition. Herein, DNA capture probes (P_1) were bound onto the amino-silanized magnetic particles to form magnetic particles-loaded P_1 (Fe_3O_4-P_1) by the glutaraldehyde cross-linking chemistry and so were the ALP-AuNCs labeled DNA detection probes (P_2) (ALP-AuNCs-P_2). As depicted in Scheme 1A, miRNA targets were captured by the prepared Fe_3O_4-P_1 and further hybridized with ALP-AuNCs-P_2. The DNA ligase-catalyzed linking was conducted for the two DNA probes complementary to miRNA targets. Moreover, the thermal treatment of incubation at 37 °C was performed followed by washings to remove or dehybridize any nonspecifically adsorbed DNA probes or mismatched miRNA targets. Then, ALP of ALP-AuNCs would hydrolyze AA-p. The resulting AA would act as a reducing agent for the reduction of Ag^+ ions, leading to the deposition of silver (Ag) on the catalytic sites of AuNCs. Subsequently, the resulting silver-deposited magnetic particles were magnetically attached onto the magnetic electrodes for electrochemical LSV measurements. A silver signal amplification-based protocol of electroanalysis was thereby proposed for probing miRNA targets.

Scheme 1B manifests the detailed experimental procedure of the silver deposition-based electroanalysis for miRNAs aided by magnetic separation. Herein, the introduction of magnetic carriers for loading DNA capture probes could facilitate the homogeneous gene hybridization and the product separations, allowing for the detection of low-level miRNAs in complex media like blood with free sample purification. The use of DNA ligase for generating the ligation between two DNA probes complementary to the short-chain miRNA targets could avoid any disconnection of the DNA detection probes during the operation steps. In the meantime, it could identify the matched miRNAs from the mismatched ones that would dehybridize after the thermal treatment at 37 °C, so that the specificity of probe-target hybridization could be ensured. More importantly, after the ligation, the ALP-AuNCs-P_2 could be firmly linked with the Fe_3O_4-P_1 to achieve higher bearing strength and capacity for larger silver accumulation toward the maximal silver signal amplification. In addition, sensitive electrochemical LSV outputs of silver signal by the Ag/AgCl solid-state voltammetric way could also help one to realize the ultrasensitive analysis of the trace-level miRNAs in blood.

Comparable Investigation of Electrochemical Responses of the Sandwiched Detection with ALP-AuNCs and DNA Ligase to Matched and Mismatched miRNAs. The electroanalysis performances of the silver deposition-based assays for miRNAs using the ALP-AuNCs-labeled detection DNA probes were investigated, in comparison to the ones labeled with native ALP (Figure 3A). It is found that the silver response of the ALP-AuNCs label (curve a) is much larger than that of the ALP label (curve b), confirming the stronger catalysis ability of the ALP-AuNCs label in amplifying the silver deposition signal toward the highly sensitive detection of

dx.doi.org/10.1021/ac5028885 | Anal. Chem. 2014, 86, 10406−10414

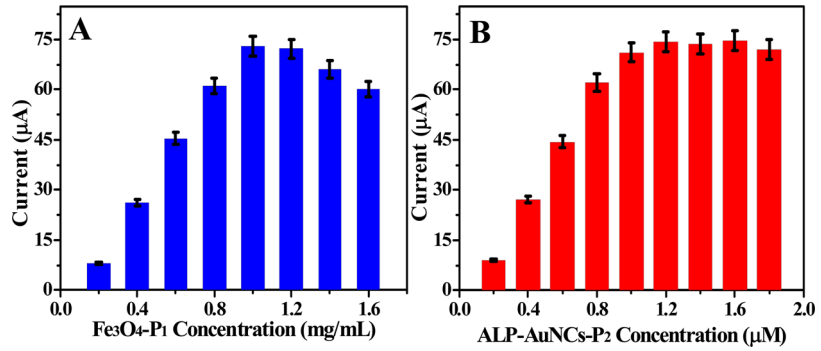

Figure 4. Effects of DNA probe concentrations on the responses of electroanalysis to miRNA targets (12.5 fM) using (A) Fe_3O_4-P_1 and (B) ALP-AuNCs-P_2 with different concentrations.

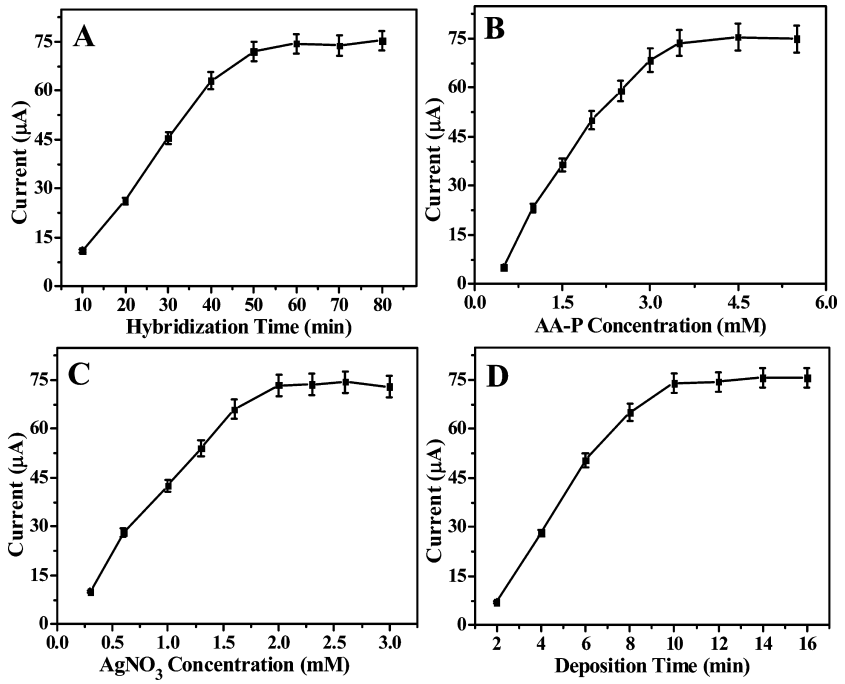

Figure 5. Optimization of the main detection conditions of (A) hybridization time, (B) AA-p substrate concentrations, (C) $AgNO_3$ dosages, and (D) the silver deposition time using an miRNA target of 12.5fM.

miRNAs. Furthermore, the key role that DNA ligase played in the catalyzing ligation of the two DNA probes after the sandwiched hybridization was also comparably studied. An evident difference in the LSV responses of silver was observed between the presence (curve a) and absence (curve c) of DNA ligase. This is described schematically in the illustrated products (inset). Herein, for the one without use of DNA ligase (curve c), the hybridized short-chain miRNA and ALP-AuNCs labeled detection DNA probe might be readily dehybridized and then detached from the magnetic carriers after the thermal treatment at 37 °C, because of the considerably low chain-melting temperature (about 21−29 °C) of two double chains so hybridized. Therefore, the use of DNA ligase could stably bridge the Fe_3O_4-P_1 and the ALP-AuNCs-P_2, so that a maximum signal amplification of silver deposition could be expected toward the ultrasensitive detection of matched miRNAs. There is one more point where the nonspecific adsorption of Ag^+ ions onto the phosphodiester backbone of single chains (curve c) and double nucleic acid chains (curves a and b) could occur, which might contribute a small LSV response of silver that is negligible as the background signal.

Moreover, the electrochemical responses of the silver deposition-based analysis method to the single-base mismatched miRNAs were examined, compared to the matched miRNAs and no target (Figure 3B). Apparently, the single-base mismatched miRNAs (curve b) showed much lower current response than the matched ones (curve a), with the response being very close to that of no target (curve c), showing a high selectivity of target hybridization. It is also confirmed visually by the photographs of the corresponding product suspensions of silver deposition reactions before the magnetic separation (inset). Therefore, the above results indicate that the developed silver deposition-based electroanalysis strategy could allow for the detection of matched miRNA targets with ultrasensitivity and high selectivity. Importantly, it can be applicable to the quantification of the mutant levels in miRNA targets on the basis of the decrease in the peak currents depending on the mutation levels.

Optimization of the Main Detection Conditions. The amount of magnetic particles-loaded DNA capture probes (Fe_3O_4-P_1) was first optimized for the electrochemical silver responses. As is shown in Figure 4A, the silver responses could

dx.doi.org/10.1021/ac5028885 | *Anal. Chem.* 2014, 86, 10406−10414

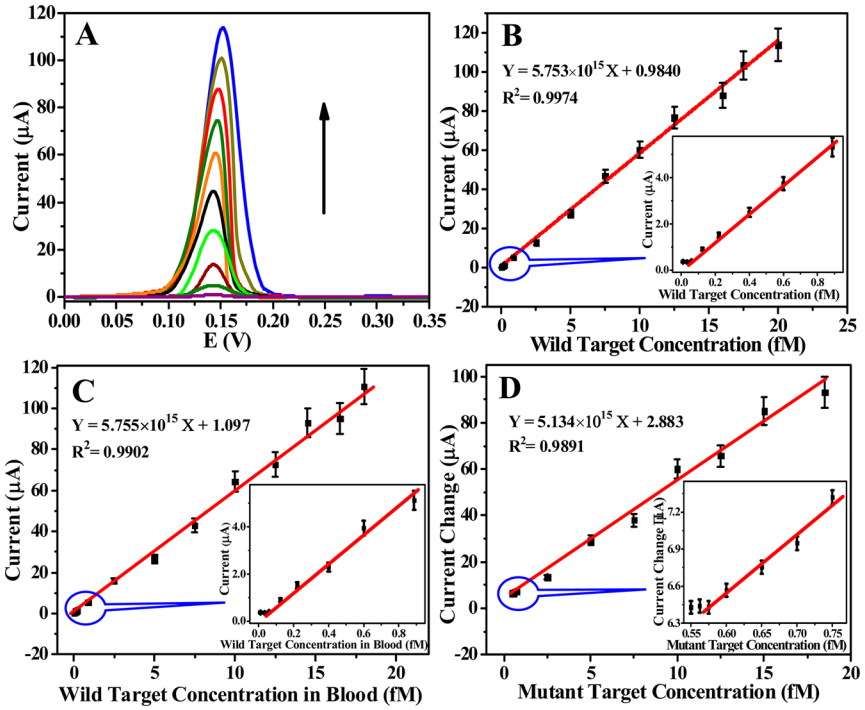

Figure 6. (A) Electrochemical LSV responses to wild miRNA samples with different concentrations (0.0050 to 20 fM). Calibration curves of the relationships between the current responses and wild miRNA samples with different concentrations spiked in (B) buffer and (C) blood. (D) The mutant-level identification of miRNAs, where the current changes were recorded for the mutant miRNAs of different concentrations spiked in wild miRNAs with the total miRNAs concentration fixed at 20.0 fM.

increase with the increasing amounts of Fe_3O_4-P_1 until 1.0 mg/mL in particles. Interestingly, too high concentrations of Fe_3O_4-P_1 might lead to the gradually decreased signals, presumably because too high density of nonconductive particles on the electrode surfaces might negatively influence their current responses. Therefore, 1.0 mg/mL of Fe_3O_4-P_1 was selected for all tests. The effects of the concentrations of ALP-AuNCs-P_2 on the silver deposition-based electroanalysis are also investigated (Figure 4B). Obviously, 1.0 μM ALP-AuNCs-P_2 is the optimum concentration for the miRNA analysis.

Moreover, the sandwiched hybridization time was explored (Figure 5A). Obviously, the peak current of deposited silver increased with the increasing reaction time and tended to be steady after 50 min, which is thus chosen for the sandwiched hybridization reaction. Furthermore, experimental investigations on the dosages of the main components in the silver deposition substrate, AA-p and $AgNO_3$, were carried out, with the data manifested in Figure 5B,C. As shown in Figure 5B, the silver signals could depend on the AA-p concentrations, of which 3.5 mM is sufficient for the silver deposition. Also, the LSV peak current increased with the increasing concentrations of $AgNO_3$ that could reach the constant responses up to 2.0 mM (Figure 5C). Herein, a sufficient silver source in the catalytic silver deposition substrate should help to prevent the diffusion of the generated AA catalyzed by ALP for the fast reduction of silver eventually deposited on the magnetic carriers. Accordingly, 3.5 mM AA-p and 2.0 mM $AgNO_3$ were adopted as the optimal substrate levels for the silver deposition reactions. In addition, the amount of deposited silver was recognized to be related to the deposition reaction time. Figure 5D displays the deposition time-dependent silver signals, showing that the silver deposition time of 10 min is enough for probing the targets with a high concentration. Notably, such a reaction time of catalytic silver deposition is much shorter than the ones without gold catalysis reported elsewhere (i.e., 30 or 35 min).[13,37] Accordingly, the introduction of AuNCs into the ALP matrix (ALP-AuNCs) as the probe labels could enhance not only the catalysis activity of ALP in the dephosphorylation reaction but also the acceleration of the silver deposition reaction to facilitate the ultrasensitive analysis of miRNAs.

Sample Analysis of Wild and Mutant miRNA Targets. Under the optimized experimental conditions, the developed silver deposition-based electroanalysis method was employed to detect the wild miRNA samples. Figure 6A shows the electrochemical LSV responses to wild miRNA targets of different concentrations in buffer. The peak currents increased with the increase in the concentrations of wild miRNA targets, where the positive shifts in the peak potentials might be associated with the increasing thickness of silver layers on the inert magnetic electrodes.[15] A linear relationship was thus obtained for the current responses versus miRNA concentrations ranging from 0.014 to 20.0 fM (R^2 = 0.9974) (Figure 6B). The detection limit is about 4.61 aM, estimated according to the 3σ rule, which is much lower than those reported previously for miRNAs such as 2.0 pM[1] and 1.0 fM.[38] Again, the ultrasensitive detection of miRNAs might presumably result from the powerful catalysis activities of bicatalytic ALP-AuNCs in catalyzing the dephosphorylation and the silver deposition reactions, aided by the DNA ligase-catalytic probe ligation as well as the sensitive electrochemical outputs aforementioned.

Moreover, the developed electroanalysis method was applied to probe the levels of wild miRNA target samples with different concentrations spiked in blood (Figure 6C). A linear detection relationship between the electrochemical responses and wild miRNA levels in blood was obtained over the miRNA

dx.doi.org/10.1021/ac5028885 | Anal. Chem. 2014, 86, 10406−10414

concentrations ranging from 0.060 to 19.0 fM (R^2 = 0.9902), with the detection limit of about 21.5 aM. In addition, the identification of the mutant levels in the miRNA samples was carried out on the basis of the decrease in the peak currents caused by the mutations (Figure 6D). Here, the current changes, which were calculated from the differences between the responses to wild miRNAs in the presence and absence of the mutant ones, were recorded for the mutant miRNAs with different concentrations spiked in wild miRNA samples with the total miRNAs fixed at 20.0 fM. Accordingly, a linear relationship was achieved for the electrochemical changes versus the mutant miRNA concentrations ranging from 0.575 to 18.0 fM (R^2 = 0.9891), with the detection limit of about 0.184 fM. The data indicate the feasibility of the identification ability of the developed method in probing the mutant levels of miRNA samples. Therefore, the developed electroanalysis strategy, which combines the ALP-AuNCs-catalytic dephosphorylation and the silver deposition, together with the DNA ligase-catalyzed ligation of specific DNA probes, could achieve the maximal signal amplification of silver deposition, thus allowing for the electrochemical detection of free wild miRNAs in blood with ultrasensitivity and high selectivity, including the identification of the single-base mutant levels in miRNA samples.

CONCLUSION

In this work, AuNCs were successfully synthesized and in-site incorporated into the protein matrix of ALP, as an example of enzymes exerting the catalysis under alkaline environment, by the protein-scaffold biomineralization route. The improved catalysis performances of ALP-AuNCs were demonstrated in the catalytic dephosphorylation and the silver deposition reactions compared to native ALP. The prepared ALP-AuNCs were labeled onto the DNA detection probes to work with magnetic particles-loaded DNA capture probes, resulting in an ultrasensitive sandwich-type detection strategy for probing short-chain miRNA targets based on the catalytic signal amplification of silver deposition. Investigation results show that AuNCs in ALP-AuNCs would act as the catalyst to accelerate the reductive silver deposition toward the rapid signal amplification for the sandwich-type detection, in addition to the enhancement of the catalysis activity of ALP in the dephosphorylation reaction. Moreover, using DNA ligase for the ligation of two DNA probes formed in the hybridization with complementary miRNA targets could ensure the maximum amplification of silver signals by the bicatalysis of ALP-AuNCs. Furthermore, the introduction of magnetic carriers to load DNA capture probes could make the hybridization reactions in a homogeneous way, especially the convenient separation operations toward the direct analysis of targets in blood. Also, the electrochemical silver outputs using the magnetic electrodes by the Ag/AgCl solid-state voltammetric process could help one to realize the sensitive signal measurements. Therefore, the developed electroanalysis method could not only probe the low-level free miRNAs in blood samples with high sensitivity and selectivity but also accurately identify the single-base mutant levels in miRNA samples. Such an electroanalysis detection method for miRNAs may hold great promise of applications in the clinical laboratory for the diagnosis of cancer and the warning of cancer metastasis.

AUTHOR INFORMATION

Corresponding Author

*E-mail: huawangqfnu@126.com. Tel: +86 537 4456306. Fax: +86 537 4456306.

Author Contributions

The manuscript was written through contributions of all authors. All authors have given approval to the final version of the manuscript.

Notes

The authors declare no competing financial interest.

ACKNOWLEDGMENTS

This work is supported by the National Natural Science Foundations of China (No. 21375075, 21302109, and 21302110), the Taishan Scholar Foundation of Shandong Province, and the Natural Science Foundation of Shandong Province (ZR2013BQ017 and ZR2013BM007), P. R. China.

REFERENCES

(1) Pohlmann, C.; Sprinzl, M. *Anal. Chem.* **2010**, *82*, 4434−4440.
(2) Ha, T. Y. *Immune Network* **2011**, *11*, 135−154.
(3) Chen, X.; Ba, Y.; Ma, L. J.; Cai, X.; Yin, Y.; Wang, K. H.; Guo, J. G.; Zhang, Y. J.; Chen, J. N.; Guo, X. *Cell Res.* **2008**, *18*, 997−1006.
(4) Nguyen, H. C. N.; Xie, W. L.; Yang, M.; Hsieh, C. L.; Drouin, S.; Lee, G. S. M.; Kantoff, P. W. *Prostate* **2013**, *73*, 346−354.
(5) Cho, W. *Int. J. Biochem. Cell Biol.* **2010**, *42*, 1273−1281.
(6) Lin, Q. F.; Mao, W. D.; Shu, Y. Q.; Lin, F.; Liu, S. P.; Shen, H.; Gao, W.; Li, S. Q.; Shen, D. *J. Cancer Res. Clin.* **2012**, *138*, 85−93.
(7) Hanash, S. M.; Baik, C. S.; Kallioniemi, O. *Nat. Rev. Clin. Oncol.* **2011**, *8*, 142−150.
(8) Wark, A. W.; Lee, H. J.; Corn, R. M. *Angew. Chem., Int. Ed.* **2008**, *47*, 644−652.
(9) Li, J.; Yao, B.; Huang, H.; Wang, Z.; Sun, C. H.; Fan, Y.; Chang, Q.; Li, S. L.; Wang, X.; Xi, J. Z. *Anal. Chem.* **2009**, *81*, 5446−5451.
(10) Driskell, J. D.; Seto, A. G.; Jones, L. P.; Jokela, S.; Dluhy, R. A.; Zhao, Y. P.; Tripp, R. A. *Biosens. Bioelectron.* **2008**, *24*, 923−928.
(11) Hwang, S.; Kim, E.; Kwak, J. *Anal. Chem.* **2005**, *77*, 579−584.
(12) Fanjul-Bolado, P.; Hernandez-Santos, D.; Gonzalez-García, M. B.; Costa-García, A. *Anal. Chem.* **2007**, *79*, 5272−5277.
(13) Qu, B.; Chu, X.; Shen, G. L.; Yu, R. Q. *Talanta* **2008**, *76*, 785−790.
(14) Lai, G. S.; Yan, F.; Wu, J.; Leng, C.; Ju, H. X. *Anal. Chem.* **2011**, *83*, 2726−2732.
(15) Feng, K. J.; Zhao, J. J.; Wu, Z. S.; Jiang, J. H.; Shen, G. L.; Yu, R. Q. *Biosens. Bioelectron.* **2011**, *26*, 3187−3191.
(16) Zhou, Y. L.; Wang, M.; Meng, X. M.; Yin, H. S.; Ai, S. Y. *RSC Adv.* **2012**, *2*, 7140−7145.
(17) Wilson, M. S. *Anal. Chem.* **2005**, *77*, 1496−1502.
(18) Wilson, M. S.; Nie, W. Y. *Anal. Chem.* **2006**, *78*, 6476−6483.
(19) Wilson, M. S.; Nie, W. Y. *Anal. Chem.* **2006**, *78*, 2507−2513.
(20) Zhou, C. H.; Zhao, J. Y.; Pang, D. W.; Zhang, Z. L. *Anal. Chem.* **2014**, *86*, 2752−2759.
(21) Liu, R.; Zhang, Y.; Zhang, S. Y.; Qiu, W.; Gao, Y. *Appl. Spectrosc. Rev.* **2014**, *49*, 121−138.
(22) Basnar, B.; Weizmann, Y.; Cheglakov, Z.; Willner, I. *Adv. Mater.* **2006**, *18*, 713−718.
(23) Berglund, G. I.; Carlsson, G. H.; Smith, A. T.; Szöke, H.; Henriksen, A.; Hajdu, J. *Nature* **2002**, *417*, 463−468.
(24) Kim, E. E.; Wyckoff, H. W. *J. Mol. Biol.* **1991**, *218*, 449−464.
(25) Stec, B.; Holtz, K. M.; Kantrowitz, E. R. *J. Mol. Biol.* **2000**, *299*, 1303−1311.
(26) Xiao, Y.; Patolsky, F.; Katz, E.; Hainfeld, J. F.; Willner, I. *Science* **2003**, *299*, 1877−1881.
(27) Yehezkeli, O.; Yan, Y. M.; Baravik, I.; Tel-Vered, R.; Willner, I. *Chem.—Eur. J.* **2009**, *15*, 2674−2679.

(28) Patolsky, F.; Weizmann, Y.; Willner, I. *Angew. Chem., Int. Ed.* **2004**, *43*, 2113−2117.
(29) Matthey, D.; Wang, J. G.; Wendt, S.; Matthiesen, J.; Schaub, R.; Lægsgaard, E.; Hammer, B.; Besenbacher, F. *Science* **2007**, *315*, 1692−1696.
(30) Lee, S.; Fan, C. Y.; Wu, T. P.; Anderson, S. L. *J. Am. Chem. Soc.* **2004**, *126*, 5682−5683.
(31) Valden, M.; Lai, X.; Goodman, D. W. *Science* **1998**, *281*, 1647−1650.
(32) Xie, J. P.; Zheng, Y. G.; Ying, J. Y. *J. Am. Chem. Soc.* **2009**, *131*, 888−889.
(33) Liu, S. H.; Xing, R. M.; Lu, F.; Rana, R. K.; Zhu, J. J. *J. Phys. Chem. C* **2009**, *113*, 21042−21047.
(34) Wang, S. M.; Su, P.; Huang, J.; Wu, J. W.; Yang, Y. *J. Mater. Chem. B* **2013**, *1*, 1749−1754.
(35) Deng, H.; Li, X. L.; Peng, Q.; Wang, X.; Chen, J. P.; Li, Y. D. *Angew. Chem., Int. Ed.* **2005**, *44*, 2782−2785.
(36) Freeman, R.; Finder, T.; Willner, I. *Angew. Chem., Int. Ed.* **2009**, *48*, 7818−7821.
(37) Qu, B.; Guo, L.; Chu, X.; Wu, D. H.; Shen, G. L.; Yu, R. Q. *Anal. Chim. Acta* **2010**, *663*, 147−152.
(38) Roy, S.; Soh, J. H.; Gao, Z. Q. *Lab Chip* **2011**, *11*, 1886−1894.